Conference on Modelling Fluid Flow (CMFF'15)
The 16th International Conference on Fluid Flow Technologies
Budapest, Hungary, September 1-4, 2015

BIFURCATION STRUCTURE OF A PERIODICALLY DRIVEN BUBBLE OSCILLATOR NEAR BLAKE'S CRITICAL THRESHOLD

Ferenc HEGEDŰS[1], Roxána VARGA[2], Kálmán KLAPCSIK[3]

[1] Corresponding Author. Department of Hydrodynamics Systems, Budapest University of Technology and Economics, Faculty of Mechanical Engineering. Műegyetem rkp. 3, H-1111 Budapest, Hungary. Tel.: +36-1-463-1680, Fax: +36-1-463-3091, E-mail: hegedusf@hds.bme.hu
[2] Department of Hydrodynamics Systems, Budapest University of Technology and Economics. E-mail: rvarga@hds.bme.hu
[3] Department of Hydrodynamics Systems, Budapest University of Technology and Economics. E-mail: kklapcsik@hds.bme.hu

ABSTRACT

It is well-known that gas/vapour bubbles in liquids growth indefinitely if the ambient pressure exceeds Blake's critical threshold. For several decades of investigations, researchers tried to find numerical evidence for the stabilization of such bubbles by applying a harmonically varying pressure field on the liquid domain (ultrasonic irradiation) in this regime, with only partial success. Since, the applied linearization on the bubble models restricted the findings only for small amplitude radial oscillations. Therefore, the present paper intends to reveal the particularly complex dynamics of a harmonically excited bubble near, but still below Blake's threshold. The computed solutions with a variety of periodicity, e.g., from period 1 up to period 9, form a well-organised structure with respect to the pressure amplitude of the excitation, provided that the applied frequency is higher than the first subharmonic resonance frequency of the bubble. This predictable behaviour provides a good basis for further investigation to find the relevant stable oscillations beyond Blake's threshold. Although, the investigated model is the very simple Rayleigh—Plesset equation, the applied numerical technique is free of the restriction of low amplitude oscillations.

Keywords: bubble dynamics, bifurcation structure, nonlinear analysis, Rayleigh—Plesset equation, ultrasonic stabilization, transient chaos

NOMENCLATURE

t	$[s]$	time
R	$[m]$	bubble radius
p	[Pa]	pressure
P	[Pa]	ambient pressure
T	[K]	ambient temperature
ρ	$[\mathrm{kg/m^3}]$	density
μ	$[\mathrm{kg/(m \cdot s)}]$	dynamic viscosity
ω	$[\mathrm{rad/s}]$	angular frequency
σ	[Nm]	surface tension
κ	ratio of the specific heats	

Subscripts and Superscripts

$\cdot$	time derivative
L	liquid
∞	far away from the bubble
A	amplitude
G	gas
V	vapour
C	critical condition
R	relative quantity
ref	reference quantity

1. INTRODUCTION

Irradiating a liquid with high frequency high intensity ultrasound, bubbles and bubble clusters are formed, called acoustic cavitation [1]. During the oscillations of the bubbles, their wall velocities can exceed thousands of $\mathrm{m/s}$ due to the inertia of the liquid domain. This phenomenon is usually called as collapse phase, and often referred to as inertial cavitation [2]. At the collapse sites, the generated extreme conditions, such as the high temperature and pressure or the induced shock wave, are exploited by various ultrasonic technological applications.

In sonochemistry, for instance, the utilization of ultrasound can increase the efficiency of various chemical reactions [3-5]. This novel technology has been spread in food and other inorganic industrial applications, in which the keen interest is to produce homogeneous mixtures from immiscible liquids, alteration of the viscosity of many food systems, increase the efficiency of heterogeneous catalysis, wastewater treatment or pasteurisation etc., see e.g. [6, 7]. Moreover, the application of ultrasound can be a new, novel and promising technology in cancer

therapy via the tissue erosion effect of acoustic cavitation [8].

Although the ultrasonic irradiation generates bubble ensembles, the study of a single spherical bubble is an important building block in both the theoretical and numerical understanding of the fundamentals of the applications. Therefore, many researchers have investigated the dynamics of a single bubble with sophisticated numerical analysis and with an increasing complexity of the physical modelling. The accumulated numerical results are summarised in many books, reviews and papers [1-2, 9-19].

The majority of the studies usually deal with liquid water at room conditions, that is, at $25\,^{o}\mathrm{C}$ ambient temperature and at $1\,\mathrm{bar}$ ambient pressure. In this case, stable bubble oscillation is ensured because of the strictly dissipative nature of physical system. At very low ambient pressure, however, such behaviour cannot be guaranteed. By lowering the pressure below the well-known Blake's critical threshold [20] the bubbles tend to grow indefinitely (without ultrasonic irradiation). This phenomenon is known as the classic cavitation.

For several decades of investigations, researchers tried to find numerical evidence for the stabilization of the bubbles by applying a harmonically varying pressure field on the liquid domain (ultrasonic irradiation) in this regime with only partial success. Since, the applied linearization on the bubble models restricted the findings only for small amplitude radial oscillations. The first significant advancement is obtained by Hegedűs [12] who could prove the existence of stably oscillating bubbles beyond Blake's threshold without any restriction in the nonlinearities. Although his result is a notable milestone, the stable solutions found correspond only to a special kind of bubble behaviour, called period 1 oscillations.

The main aim of the present paper is to reveal the complex dynamics of a harmonically excited spherical air/vapour bubble placed in water near, but still below Blake's threshold. The found solutions show a variety of periodicity, e.g., from period 1 up to period 9, which form a well-organised structure with respect to the pressure amplitude of the excitation, provided that the applied frequency is higher than the first subharmonic resonance frequency of the bubble. This predictable behaviour provides a good basis to extend the already acquired understanding by Hegedűs [12] from period 1 solutions to oscillations with arbitrary periodicity beyond the critical threshold. Although the applied model is the simple Rayleigh—Plesset equation, the employed numerical technique does not involve linearization or other reduced order modelling. Therefore, the presented technique can be easily extended for more complex models with high amplitude oscillations.

2. THE BUBBLE MODEL

The bubble model governing the evolution of the bubble radius is the simple well-known Rayleigh—Plesset equation [9] written as

$$R\ddot{R} + \frac{3}{2}\dot{R}^2 = \frac{1}{\rho_L}(p_L - p_\infty), \tag{1}$$

where the dot stands for the derivative with respect to time, $R(t)$ is the time dependent bubble radius, ρ_L is the density of the liquid water. The pressure at the bubble wall in the liquid side is p_L and far away from the bubble

$$p_\infty(t) = P_\infty + p_A\, sin(\omega t) \tag{2}$$

is a sum of the static ambient pressure P_∞ and the harmonic driving with pressure amplitude p_A and angular frequency ω. The relationship between the pressure inside and outside the bubble at its wall is defined by the mechanical balance:

$$p_G + p_V = p_L + \frac{2\sigma}{R} - 4\mu_L\frac{\dot{R}}{R}. \tag{3}$$

Here, the total pressure inside the bubble is the sum of the non-condensable gas pressure p_G and vapour pressure p_V. The vapour pressure was constant during the simulations, but it depended on the constant ambient temperature. The surface tension is σ and the liquid kinematic viscosity is μ_L. The air inside the bubble follows a simple adiabatic state of change written in the form according to [12]:

$$p_G = \left(\frac{2\sigma}{3\kappa R_C}\right)\left(\frac{R_C}{R}\right)^{3\kappa}, \tag{4}$$

where R_C is the equilibrium bubble radius of the unexcited system ($p_A = 0$) at Blake's threshold (see the detailed explanation below) and $\kappa = 1.4$ is the ratio of the specific heats for diatomic gas content.

In the bubble model, we assume that the water contains some amount of dissolved gas. The seeds or nuclei-sites, which can be pre-existing gas micro bubbles, are the week points of the liquid where the acoustic cavitation can be initiated. The mass of gas inside the bubble than can grow by rectified diffusion forming larger gas/vapour bubbles [21]. The process of rectified diffusion has orders of magnitude larger time scale than the period of the acoustic forcing.

It is important to emphasize that the constant vapour pressure and adiabatic state of change for the gas content is a severe assumption [22]. In the present study, however, the main aim is to reveal the topology of the stable periodic solutions rather than the precise physical description. This simple model allows to perform detailed parameter studies, which were essential in the understanding of the topology. Moreover, many other oscillators in different branches of science have the same/similar topological description implying that the found structure is universal in harmonically excited systems. Therefore, we expect the same qualitative behaviour for more complex bubble models, as well.

1.1. Equilibrium radius of the unexcited system

The equilibrium bubble radius curve of the unexcited system ($p_A = 0\ Pa$) is presented in Fig. 1 at ambient temperature $T_\infty = 37\ ^oC$, and computed by means of Eqs. (1) to (4) by setting all the time derivatives to zero. The stable R_E^s and the unstable R_E^u equilibrium radii are represented by the black and red curves, respectively. The two kinds of long-term behaviour are separated by the Blake's critical conditions marked by the dot in Fig. 1, where the curve turns back and tends to infinity as the tension approaches to zero.

According to [12], the critical condition can be characterised by its critical equilibrium radius set to be $R_C = 0.1\ mm$, which is the upper limit of the typical nuclei size in water [9]. Then, the critical tension can be formulated as

$$p_V - P_C = \frac{2\sigma}{R_C}\frac{3\kappa - 1}{\kappa} = 1067\ Pa. \tag{5}$$

By defining a dimensionless relative pressure as

$$P_R = \frac{p_V - P_\infty}{p_V - P_C}, \tag{6}$$

three main region can be distinguished in the horizontal axis. If $P_R < 0$ there is only one stable equilibrium radius, the system is strictly dissipative and all the trajectories tend to this sole stable behaviour. In case of $0 < P_R < 1$, an unstable fix point appears beside the stable one. In spite of the existence of stable long-term behaviour, stable oscillations cannot be guaranteed in this parameter domain, and bubbles may grow to infinity for a given set of initial conditions. Above $P_R = 1$ (beyond Blake's threshold), equilibrium radii are completely absent. Regardless of the initial conditions, it is impossible to obtain stable oscillation. Again, this region was the keen interest by many researchers to find evidence for the stabilization mechanism of harmonic forcing discussed in more detail in the Introduction.

Although Hegedűs [12] have already find the evidence for the existence of stable solutions, it is restricted only to period 1 oscillations. In his work, the crucial starting point was the exploration of all the stable period 1 solutions in the pressure amplitude p_A – frequency ω parameter plane at relative pressure $P_R = 0.9$.

Therefore, the main aim of the present study is to reveal and explore the structure and organization of the periodic solutions at the same relative pressure (0.9) marked by the blue vertical line in Fig. 1. This means that the ambient pressure is $P_\infty = 5458\ Pa$. The obtained topological description is an important progress toward the extension of the numerical results beyond Blake's threshold from period 1 solution to arbitrary periodicity.

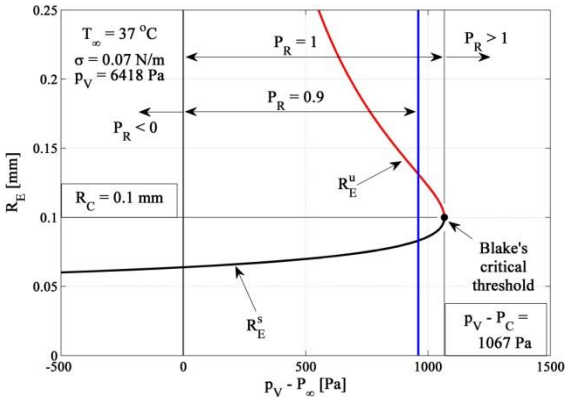

Figure 1. Equilibrium bubble radius curve as a function of the tension $p_V - P_\infty$ at ambient temperature $T_\infty = 37\ ^oC$. The solid black and red curves are the stable and unstable equilibrium radii, respectively. The black dot denotes Blake's critical threshold.

1.2. Dimensionless quantities and parameter values

Throughout the paper, dimensionless quantities were used for better numerical behaviour, such as, dimensionless time:

$$\tau = \frac{\omega t}{(2\pi)}. \tag{7}$$

Observe that in the dimensionless system the period of the excitation becomes unity $\tau_o = 1$. The dimensionless bubble radius and wall velocity are

$$y_1 = \frac{R}{R_C} \tag{8}$$

and

$$y_2 = \frac{2\pi\dot{R}}{R_C\omega}, \tag{9}$$

respectively. Finally, the relative frequency is defined as

$$\omega_R = \frac{\omega}{\omega_{ref}}, \tag{10}$$

where the reference frequency, according to [12], is

$$\omega_{ref} = \sqrt{\frac{4\sigma}{\rho_L R_C^3}} = 16793\,\frac{rad}{s}. \tag{11}$$

The values of the applied parameters and material properties are summarized in Table 1. The liquid properties are calculated from the Haar—Galagher—Kell equation of state [23] with $P_\infty = 5458\ Pa$. and with $T_\infty = 37\ ^oC$.

Table 1. Values of the applied parameters and material properties

Property	Value
Ambient pressure P_∞	5458.3 Pa
Ambient temperature T_∞	$37\ ^oC$
Surface tension σ	$0.07\ N/m$
Liquid density ρ_L	$993.13\ kg/m^3$

Liquid dyn. viscosity μ_L	$6.858 \cdot 10^{-4}\ \frac{kg}{m \cdot s}$
Vapor pressure p_V	$6418.8\ Pa$
Bubble size R_C	$0.1\ mm$
Relative pressure P_R	0.9
Pressure amplitude p_A	$0\ kPa - 10\ kPa$
Excitation frequency ω_R	$0.1 - 5$

2. RESULTS AND DISCUSSION

The simplest and still widely used method to find stable oscillations is to take an initial value problem solver and integrate system (1) to (4) forward in time by applying suitable initial conditions $y_1(0)$ and $y_2(0)$. After the convergence to a stable solution (attractor), some characteristic properties of the found solution are recorded. For instance, the points of the Poincaré map (see the detailed description later), the maximum bubble radius and wall velocity of the bubble oscillation, the largest Lyapunov exponent to reveal the existence of chaotic attractor or the periodicity in case of periodic orbits. In the following, with this simple method, the stable solutions will systematically be explored as a function of the pressure amplitude p_A and excitation frequency ω.

1.2. Unique features of the oscillations

Due to the non-strictly dissipative nature of the system, the hunting for stable oscillations is not trivial. Figure 2 shows two examples for a stable (black curve) and for an unstable (red curve) transient trajectory by applying relatively close initial conditions. Keep in mind that the period of the excitation of the dimensionless system τ_o is unity, therefore, the integer values of the horizontal axis represents integer number of acoustic cycles. Consequently, after surviving approximately 8 cycles, the unstable solution starts to diverge exponentially from the stable one, and tends to grow infinitely.

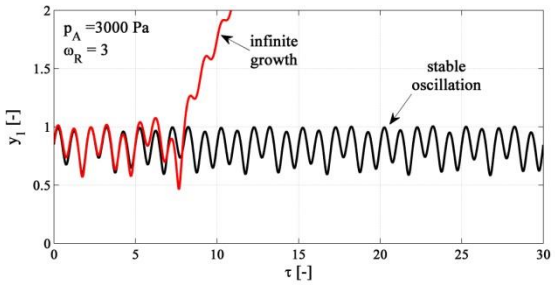

Figure 2. Dimensionless bubble radius vs. time curves for a stable bubble oscillation (black curve) and for an unstable transient solution (red curve).

The technique to overcome this difficulty is to apply several randomized initial conditions. The more the number of the initial conditions the greater the probability to find stable orbits. During the numerical calculations, 20 initial conditions were used at a given parameter combination. As a by-product, this method is capable to explore the co-existence of the different kind of attractors. Figure 3 represents three kind of stable periodic solutions at pressure amplitude $p_A = 2556\ Pa$ and at relative frequency $\omega = 5$. Observe that the periods of the oscillations are equal to (black), 7 times (blue) and 21 times (red) the period of driving. In the language of nonlinear dynamics, these solutions are called period 1, 7 and 21 attractors, respectively. Such co-existence is a clear evidence for the non-linear nature of the bubble oscillator.

The periodic orbits in the state space, y_1-y_2 plane, form closed curves, see the lower panel of Fig. 3. Because of the time dependent harmonic forcing, the trajectories in this plane can intersect themselves demonstrated by the blue curve corresponding to the period 7 orbit. Therefore, in the forthcoming diagrams, only the points of the Poincaré section will be presented, which are obtained by sampling the continuous solutions with the period of the driving. This technique is very common in periodically driven non-linear systems [24]. Observe that the trajectory of the period 21 solution is omitted, and only the 21 number of red Poincaré points are depicted in order to avoid overcrowding of the figure.

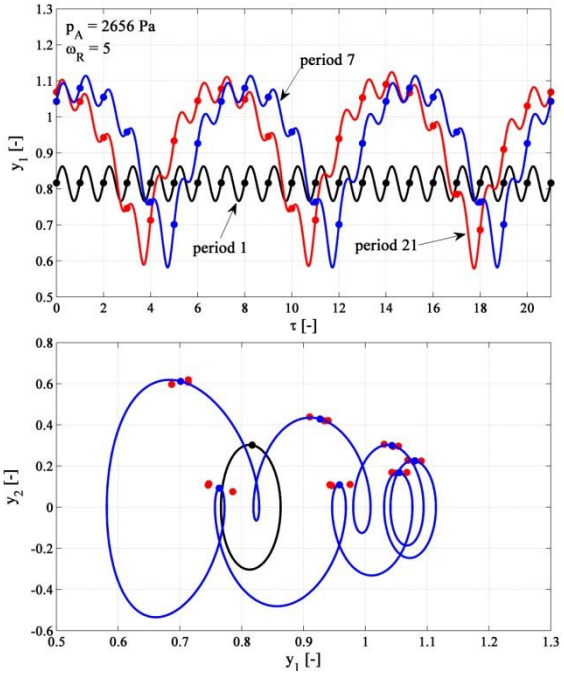

Figure 3. Co-existing stable period 1 (black), period 7 (blue) and period 21 (red) attractors. Upper panel: dimensionless bubble radius vs. times curves. Lower panel: trajectories in the state space. The dots are the points of the Poincaré section.

Another interesting feature of the system is the presence of transient chaos [25], which further complicates the finding of stable bubble motions. Such oscillations are chaotic, but they are unstable in nature. Therefore, they are extremely difficult to find. Integrating the system backward in time cannot solve the problem either, as they are usually related to chaotic saddles. The appearances of solutions with a relatively long seemingly stable behaviour which finally become unstable as the time tends to infinity are good indicators for the existence of a chaotic saddle. An example for such transient bubble oscillation is presented in Fig. 4, where the solution seems to be stable up to 80 acoustic cycles.

The determination of some characteristic properties, such as the largest Lyapunov exponent, fractal dimension etc., of the transient chaos needs huge number of numerical computations. A typical technique, for instance, is to measure the escape rate of several trajectories, initiated randomly [25]. Although the method is relatively simple, for sufficient precision, the application of millions of initial conditions is usually required.

During the numerical computations, the maximum number of allowed acoustic cycles were 1500. After this, the solution was regarded as stable chaos provided that its Lyapunov exponent was positive. If the Lyapunov exponent is negative and the solution does not converged until 1500 cycles, then the solution was discarded.

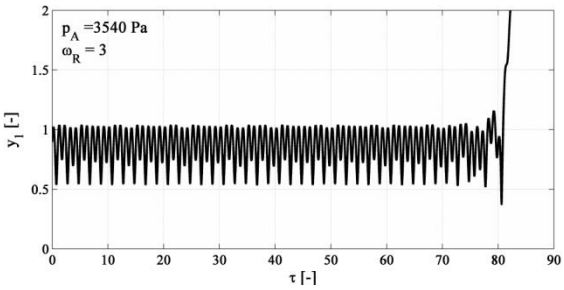

Figure 4. Unstable solutions with a very long seemingly stable behaviour indicating the presence of transient chaos.

1.2. Topological structure of the periodic attractors

A more condensed representation of the behaviour of the bubble is the bifurcation diagram, where a particular property of the found attractors, e.g. the maximum of the bubble radius or a single component of the Poincaré section, is presented as a function of a parameter. In Fig. 5. the first co-ordinate of the Poincaré section $P(y_1)$ is plotted against the pressure amplitude p_A at $\omega_R = 1$. The periodicities of the found attractors are marked by arabic numbers.

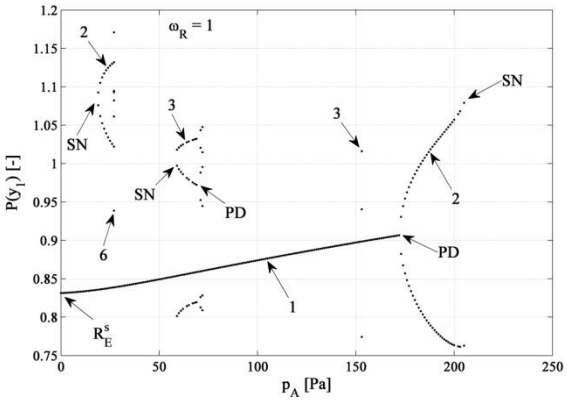

Figure 5. Example for a bifurcation diagram, that is, the first component of the Poincaré section is presented as a function of the pressure amplitude p_A as control parameter at relative frequency $\omega_R = 1$.

From the stable equilibrium radius R_E^S of the unexcited system, a stable period 1 solution emerges as the pressure amplitude is started to increase from $p_A = 0\ Pa$. It becomes unstable at $p_A = 172\ Pa$ and a new period 2 attractor comes to existence through a period doubling (PD) bifurcation. This period doubled solution turns back and become unstable at approximately $p_A = 205\ Pa$ via a saddle-node (SN) bifurcation. The unstable branch (computed in [13] for a similar structure) turns back again via an SN bifurcation at $p_A = 19\ Pa$ establishing a period 2 attractor co-existing with the former period 1 stable solution.

Observe that in a relatively wide parameter range a period 3 attractor emerges via an SN bifurcation and go through a PD bifurcation. Such co-existence of the attractors is a common feature of non-linear systems.

In order to get a global picture about the relevant periodic attractors in the pressure amplitude p_A - relative frequency ω_R parameter plane, a series of bifurcation diagrams were computed and presented in Fig. 6, similar to that of demonstrated in Fig. 5. As the relative frequency is increased from 2 to 5 a remarkably complex and intriguing structure is being evolved.

At relative frequency $\omega_R = 2$ (Fig. 6A), the main bifurcation structure is formed by the period 1, 2, 3, 4 and 5 solutions. Their organisation seems to follow a simple rule, namely, between the appearance of two solutions with period X and Y, there is another one with period $X + Y$. Observe, for instance, that between the period 3 and 2 attractors there is a period 5 stable solution, as well. Further increasing the relative frequency, the obtained results strongly supports this structural description, see Fig. 6B to Fig. 6D. Gradually, more and more attractors, up to period 9, emerge through SN bifurcations towards the negative pressure amplitudes, whose periodicities obey the aforementioned simple rule.

This topological description in terms of the periodicity is summarised by a pictogram in Fig. 7 up to level four. In the literature, this organisation is called as Farey-ordering, and it seems to a universal rule describing the topology of the stable solutions in many dynamical systems [26-30].

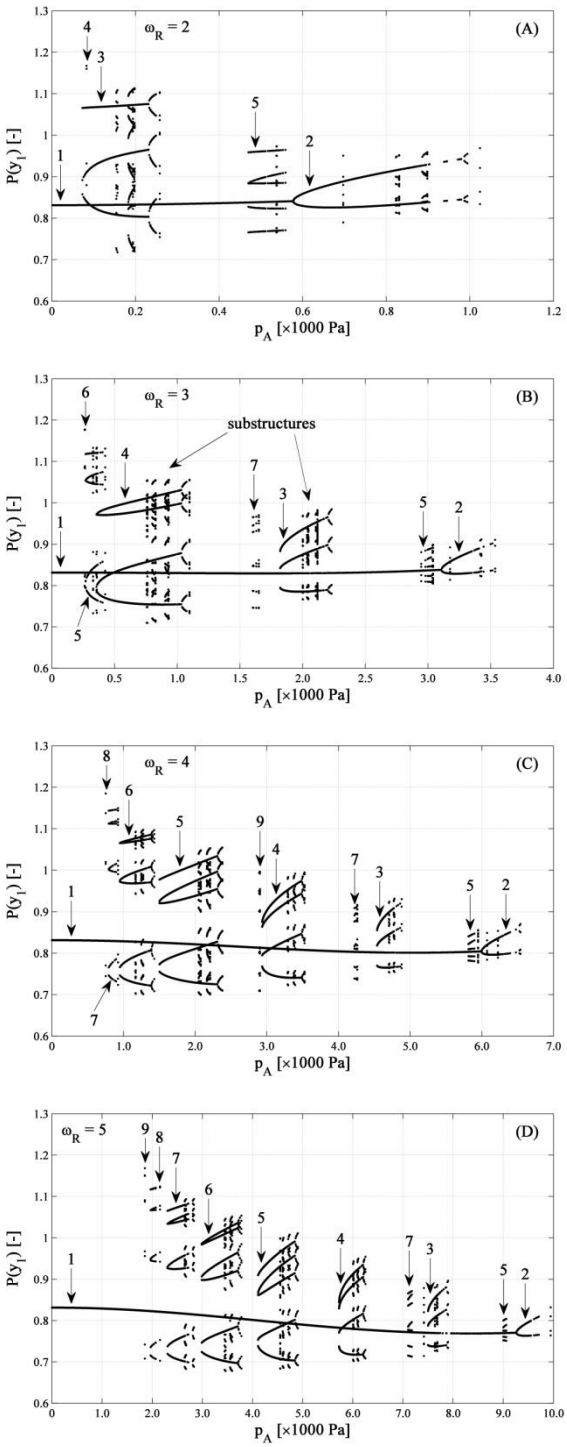

Figure 6. Series of bifurcation diagrams with the pressure amplitude p_A as control parameter at different relative frequencies ω_R.

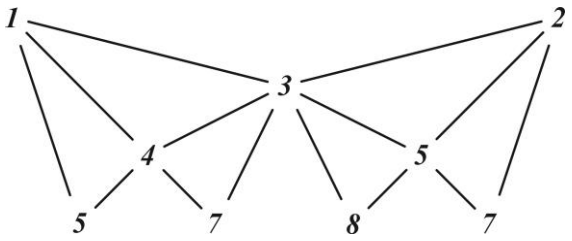

Figure 7. Organisation structure of the periodic attractors as a function of the pressure amplitude p_A as control parameter in terms of periodicity above relative frequency $\omega_R > 2$.

It should be noted, that a fine co-existing substructure exists for each periodic attractor, see e.g. the stable solutions with very high periodicities in the range of period 4 and 3 solutions in Fig. 6.B. The analysis of these attractors is out of the scope of the present investigation.

5. SUMMARY

In case of a spherical gas/vapour bubble, at constant, but sufficiently low ambient pressure (beyond Blake's critical threshold) equilibrium radius does not exist and the bubble tends to grown indefinitely. In this parameter region, Hegedűs [12] could find evidence for stable bubble oscillation by applying harmonically varying pressure filed on the liquid domain, however, only for a special, period 1 solutions. In order to extend this knowledge to arbitrary periodicity, this paper focuses on the topological description of the stable solutions at low, but still above the critical threshold. The results show that organisation of the attractors follows a simple rule characterised by the well-known Farey-ordering. This finding is vital and necessary to leap forward, and obtain a good theoretical understanding for the stabilization mechanism for ambient pressures beyond Blake's critical threshold.

The mathematical model was the simple Rayleigh—Plesset equation, which is a second order non-linear ordinary differential equation. The size of the applied bubble was 0.1 mm placed in liquid water.

ACKNOWLEDGEMENTS

This work has been supported by the Hungarian National Fund for Science and Research under contract No. OTKA K81621.

REFERENCES

[1] Leighton, T. G., 1994, *The Acoustic Bubble*, Academic, London.

[2] Young, F. R., 1989, *Cavitation*, McGraw-Hill, London.

[3] Merouani, S., Hamdaoui, O., Rezgui, Y., and Guemini, M., 2013, "Effects of ultrasound frequency and acoustic amplitude on the size of

sonochemically active bubbles – Theoretical study", *Ultrason Sonochem*, Vol. 20, pp. 815-819.

[4] Brotchie, A., Mettin, R., and Grieser, F., 2009, "Cavitation activation by dual-frequency ultrasound and shock waves", *Phys Chem Chem Phys*, Vol. 11, pp. 10029-10034.

[5] Prabhu, A. V., Gogate, P. R., and Pandit, A. B., 2004, "Optimization of multiple-frequency sonochemical reactors", *Phys Chem Eng Sci*, Vol. 59, pp. 4991-4998.

[6] Knorr, D., Zenker, M., Heinz, V. and Lee, D.-U., 2004, "Applications and potential of ultrasonics in food processing", *Trends Food Sci Tech*, Vol. 15, pp. 261-266.

[7] Patist, A., and Bates, D., 2008, "Ultrasonic innovations in the food industry: From the laboratory to commercial production", *Innov Food Sci Emerg Technol*, Vol. 9, pp. 147-154.

[8] Kennedy, J. E., Haar, G. R. and Cranston, D., 2014, "High intensity focused ultrasound: surgery of the future?", *Brit J Radiol*, Vol. 76, pp. 590-599.

[9] Brennen, C. E., 1995, *Cavitation and Bubble Dynamics*, University Press, Oxford.

[10] Feng, Z. C., and Leal, L. G., 1997, "Nonlinear bubble dynamics", *Annu Rev Fluid Mech*, Vol. 29, pp. 201-243.

[11] Lauterborn, W., and Kurz, T., 2010, "Physics of bubble oscillations", *Rep Prog Phys*, Vol. 73, pp. 106501.

[12] Hegedűs, F., 2014, "Stable bubble oscillations beyond Blake's critical threshold", *Ultrasonics*, Vol. 54, pp. 1113-1121.

[13] Hegedűs, F., Hős, C., and Kullmann, L., 2013, "Stable period 1, 2 and 3 structures of the harmonically excited Rayleigh—Plesset equation applying low ambient pressure", *IMA J Appl Math*, Vol. 78, pp. 1179-1195.

[13] Hegedűs, F., and Kullmann, L., 2012, "Basin of attraction in a harmonically excited bubble model", *Period. Polytech Mech Eng*, Vol. 56, pp. 125-132.

[14] Sojahrood, A. J., and Kolios, M. C., 2012, "Classification of the nonlinear dynamics and bifurcation structure of ultrasound contrast agents excited at higher multiples of their resonance frequency", *Phys Lett A*, Vol. 376, pp. 2222-2229.

[15] Behnia, S., Sojahrood, A. J., Soltanpoor, W., and Jahanbakhsh, O., 2009, "Nonlinear transitions of a spherical cavitation bubble", *Chaos Soliton Fract*, Vol. 41, pp. 818-828.

[16] Behnia, S., Sojahrood, A. J., Soltanpoor, W., and Jahanbakhsh, O., 2009, "Nonlinear transitions of a spherical cavitation bubble", *Chaos Soliton Fract*, Vol. 41, pp. 818-828.

[17] Behnia, S., Sojahrood, A. J., Soltanpoor, W., and Sarkhosh, L., 2009, "Towards classification of the bifurcation structure of a spherical cavitation bubble", *Ultrasonics*, Vol. 49, pp. 605-610.

[18] Behnia, S., Sojahrood, A. J., Soltanpoor, W., and Jahanbakhsh, O., 2009, "Suppressing chaotic oscillations of a spherical cavitation bubble through applying a periodic perturbation", *Ultrason Sonochem*, Vol. 16, pp. 502-511.

[19] Parlitz, U., Englisch, V., Scheffczyk, C., and Lauterborn, W., 1990, "Bifurcation structure of bubble oscillators", *J Acoust Soc Am*, Vol. 88, pp. 1061-1077.

[20] Blake, F. G., 1949, "The onset of cavitation in liquids: I.", *Acoustic Res Lab, Harvard Univ Tech Memo*, No. 12.

[21] Fyrillas, M.M., Szeri, A. J., 1994, "Dissolution or growth of soluble spherical oscillating bubbles", *J Fluid Mech*, Vol. 277, pp. 381-407.

[22] Plesset, M.S., Prosperetti, A., 1977, "Bubble dynamics and cavitation", *Ann Rev Fliud Mech*, Vol. 9, pp. 145-185.

[23] Haar, L., Gallagher, J. S., and Kell, G. S., 1988, *NBS/NRC Wasserdampftafeln*, Springer, Berlin.

[24] Kuznetsov, Y. A., 2004, *Elements of Applied Bifurcation Theory*, Springer, New York.

[25] Lai, Y.-C., and Tél, T., 2010, *Transient Chaos: Complex Dynamics on Finite-Time Scales*, Springer, New York.

[26] Gilmore, R., and McCallum, J. W. L., 1995, "Structure in the bifurcation diagram of the Duffing oscillator", *Phys Rev E*, Vol. 51, pp. 935-956.

[27] Goswami, B. K., 1998, "Self-similarity in the bifurcation structure involving period tripling, and a suggested generalization to period *n*-tupling", *Phys Lett A*, Vol. 245, pp. 97-109.

[28] Gilmore, R., 1998, "Topological analysis of chaotic dynamical systems", *Rev Mod Phys*, Vol. 70, pp. 1455-1529.

[29] Cvitanović, P., and Myrheim, J., 1983, "Universality for period n-tuplings in complex mappings", *Phys Lett A*, Vol. 94, pp. 329-333.

[30] Englisch, V., and Lauterborn, W., 1994, "The winding-number limit of period-doubling

cascades derived as Farey-fraction", *Int J Bifurcat Chaos*, Vol. 4, pp. 999-1002.